

## Low-Temperature Properties of the Heavy-Fermion Compound $\text{CeRu}_2\text{Si}_2$ at the Metamagnetic Transition

C. Paulsen, A. Lacerda, L. Puech, P. Haen, P. Lejay, J. L. Tholence, and J. Flouquet

Centre de Recherches sur les Très Basses Températures, C.N.R.S., Grenoble-Cédex, France

and

A. de Visser

Natuurkundig Laboratorium, Universiteit van Amsterdam, Amsterdam, The Netherlands

(Received July 18, 1990)

*Magnetization measurements performed below 1 K on a single-crystalline sample of the heavy fermion compound  $\text{CeRu}_2\text{Si}_2$  are reported. The field variation of the linear term of the specific heat  $\gamma$  derived from these data (via a Maxwell relation) exhibits a large peak at the metamagnetic-like transition at  $B^*$  ( $=7.7$  at  $T \rightarrow 0$ ). Thermal-expansion measurements, show a drastic drop of the temperature where a Fermi liquid behavior is reached when  $B \rightarrow B^*$ . Similar experiments performed on a single-crystalline  $\text{Ce}_{0.95}\text{La}_{0.05}\text{Ru}_2\text{Si}_2$  sample show a broadening of all the anomalies at  $B^*$  and a reduction of their intensities. These results strongly suggest that pure  $\text{CeRu}_2\text{Si}_2$  approaches a magnetic instability at  $B^*$  for  $T \rightarrow 0$ .*

### 1. INTRODUCTION

One of the key points in heavy-fermion problems is to understand the connection between magnetism and electronic properties. The most interesting heavy-fermion compounds are located in the vicinity of a magnetic instability, i.e., applying external variables as pressure  $P$  or magnetic field  $B$  gives the possibility of a transit from a long-range magnetic ordered (generally antiferromagnetic (AF)) to a Pauli-paramagnetic (PP) ground state. Furthermore, the applied magnetic field will drive volume  $V$  changes.

So the interplay is not only limited to magnetic and low-energy electronic excitations but can also involve a lattice instability. The low characteristic temperature  $T^*$  of the heavy-fermion ground state leads to huge effective masses  $m^*$ , but also to unusual large volume Grüneisen coefficients<sup>1</sup>  $\Gamma = -\partial \ln T^*/\partial \ln V$ . One of the best proofs of strong renormalization effects is that both quantities ( $m^*$ ,  $\Gamma$ ) are strongly enhanced in heavy-fermion compounds, but that their ratio ( $\Gamma/m^*$ ) never exceeds by more than one order of magnitude the value obtained either for free electrons or for the Fermi liquid <sup>3</sup>He (Ref. 2). The large magnitude of  $\Gamma$  will magnify any small volume change  $\delta V$  and thus may be equivalent in usual solids to a fictitious huge volume change ( $\Gamma\delta V/V$ ). In many solids, a volume variation of a few percent induces a drastic change in electronic and lattice properties. For  $\Gamma \sim 100$ , one may expect similar transitions for a bare volume change near  $10^{-3}$ . Such a variation can be easily induced by pressure (a few kilobar) or by a magnetic field through magnetostriction effects.

In order to corroborate this, we present here an illustrating study based on magnetization, magnetostriction, and thermal-expansion experiments, performed on  $\text{CeRu}_2\text{Si}_2$  well below 1 K.  $\text{CeRu}_2\text{Si}_2$  is a heavy-fermion compound characterized by a coefficient  $\gamma = 350 \text{ mJ mol}^{-1} \text{ K}^{-2}$  of the linear contribution  $C = \gamma T$  to the specific heat.<sup>3,4</sup> Up to now, no small ordered moments have been detected in  $\text{CeRu}_2\text{Si}_2$ , contrary to the cases of  $\text{UPt}_3$  and  $\text{URu}_2\text{Si}_2$ .  $\text{CeRu}_2\text{Si}_2$  is thus considered to have a PP ground state. It also does not become superconducting down to 20 mK (Ref. 5). However,  $\text{CeRu}_2\text{Si}_2$  is close to a magnetic transition (from PP to AF) as shown by the large value of its Grüneisen parameter<sup>6,7</sup> and by the observation<sup>8</sup> that replacing 8% of the Ce atoms by lanthanum atoms leads to a long-range order.

As other heavy fermion compounds, like  $\text{UPt}_3$  and  $\text{URu}_2\text{Si}_2$ ,  $\text{CeRu}_2\text{Si}_2$  shows a large positive nonlinearity of its magnetization  $M$  for  $B$  applied along the easy direction. This means that the differential susceptibility,  $\chi = \partial M/\partial B$ , shows a well-defined maximum at a critical field  $B^* \sim 8 \text{ T}$ . In  $\text{CeRu}_2\text{Si}_2$ , this effect occurs for  $B$  parallel to the tetragonal  $c$  axis and becomes clearly discernable<sup>5</sup> below 15 K. Referring to  $B^*$  as a metamagnetic field seems to be justified by the observation<sup>9</sup> of short-range magnetic intersite correlations that collapse in the vicinity of  $B^*$ .

The particularly interesting aspects of  $\text{CeRu}_2\text{Si}_2$  are that (i) the crystal field doublet ground state is well isolated from the first excited level<sup>3</sup> (220 K) and (ii) the low value of  $B^*$ , when compared to the large values in  $\text{UPt}_3$  (20 T) (Ref. 10) and in  $\text{URu}_2\text{Si}_2$  (>30 T) (Ref. 11) allows for macroscopic measurements and microscopic neutron-scattering experiments. The leading role of the sample homogeneity (connected to the itinerancy of the quasi particles) is demonstrated by comparing  $\text{CeRu}_2\text{Si}_2$

with  $\text{Ce}_{0.95}\text{La}_{0.05}\text{Ru}_2\text{Si}_2$ , that also has a PP ground state with a metamagnetic field  $B^* \sim 5.3$  T.

## 2. EXPERIMENTAL DETAILS

Single-crystalline samples of  $\text{CeRu}_2\text{Si}_2$  and  $\text{Ce}_{0.95}\text{La}_{0.05}\text{Ru}_2\text{Si}_2$  were grown by the Czochralski technique in a three-arc furnace. High-purity elements Ce(99.99%), Si(>99.999%) and La(99.99%), supplied by Johnson-Matthey, and Ru(99.999%), supplied by Leico Ind. Inc., were used. The samples were shaped by means of spark erosion, into parallelepipeds with edges  $\sim 3$ –5 mm.

The magnetization measurements were made using a miniature dilution refrigerator and a high-field, low-temperature SQUID magnetometer developed at the CRTBT. The bottom part of the vacuum jacket of the dilution refrigerator is made of a leak-tight quartz tube, which fits into an 8 T magnet. The pick-up coils are located in liquid He, in the space between the quartz tube and the superconducting magnet. A long copper tress holding the sample is attached to the cold finger of the mixing chamber. The sample is placed in one of the pick-up coils. The lowest temperature amounted to  $T_0 = 150$  mK and 200 mK, for  $\text{Ce}_{0.95}\text{La}_{0.05}\text{Ru}_2\text{Si}_2$  (Ref. 12) and  $\text{CeRu}_2\text{Si}_2$  (Ref. 13) respectively. The magnetization difference  $\Delta M = M(T) - M(T_0)$  at constant field was measured for a large number of temperatures and fields. Even in 8 T differences in  $\Delta M$  of  $10^{-6} \mu\text{B}/\text{Ce}$  could be detected.

The coefficient of linear thermal expansion,  $\alpha = L^{-1}(dL/dT)$ , and linear magnetostriction,  $\lambda' = L^{-1}(dL/dB)$ , were measured using a sensitive three-terminal capacitance method. The samples were mounted in a parallel-plate capacitance cell, machined out of OFHC (oxygen-free high-conductivity copper), similar to that described in Ref. 14. Measurements in the temperature range  $1.3 \text{ K} \leq T \leq 20 \text{ K}$ , partially reported in Refs. 15 and 16, have been performed in a variable temperature cryostat. The temperature of the cell was measured with a carbon-glass thermometer, previously calibrated in several magnetic fields, with an accuracy of 0.01 K. Fields up to 8.5 T could be achieved in pumped helium. Data points were collected by stabilizing the temperature step by step.

Measurements below 1.2 K were performed on  $\text{CeRu}_2\text{Si}_2$  in a dilution refrigerator equipped with a 12 T superconducting solenoid. The temperature of the mixing chamber can be stabilized by a heater and measured with a sliced speer-carbon thermometer. The capacitance cell was thermally anchored to the mixing chamber via a rigid copper support. A second set of heater and carbon thermometer were attached close to the cell. This thermometer was calibrated in field by comparing with the one that was placed in the field compensated region of the mixing chamber. The data

points were obtained as previously, by heating the cell stepwise, while recording the corresponding capacitance variations. The lowest temperature amounted to 80 mK. Experiments on  $\text{Ce}_{0.95}\text{La}_{0.05}\text{Ru}_2\text{Si}_2$  were performed in the temperature range  $0.35 \text{ K} \leq T \leq 1.5 \text{ K}$  with the capacitance cell attached to the cold plate of a  $^3\text{He}$  cryostat. The maximum field available here was 8 T. The temperature of the cell was measured by means of a ruthenium oxide thermometer previously calibrated in fields. In both experiments the detection limit was  $0.1 \text{ \AA}$ .

### 3. RESULTS

#### 3.1. Magnetization

Previous magnetization measurements,<sup>5,15</sup> performed above 1.3 K by an extraction method, have shown that the differential susceptibility at  $B^*$ ,  $\chi(B^*) = dM/dB|_{B^*}$ , obeys a Curie-Weiss law with small  $\theta$  values, while the initial susceptibility  $\chi(0)$  has already reached a low temperature  $T^2$  behavior. Recent ac-susceptibility measurements<sup>17</sup> performed at low temperature show for  $x=0$  a flattening of  $\chi(B^*)$  only below 200 mK. In Figs. 1 and 2 we present the magnetization differences  $\Delta M = M(B) - M(B^*)$  as a function of  $T^2$  for several values of  $B$ , for  $\text{CeRu}_2\text{Si}_2$  and  $\text{Ce}_{0.95}\text{La}_{0.05}\text{Ru}_2\text{Si}_2$ , respectively. The conversion of the relative  $\Delta M$  value of the raw data into the absolute  $\Delta M$  scale of Figs. 1 and 2 could be made by comparing these data with the absolute magnetization values measured by an extraction method. A  $T^2$  variation is observed for  $x=0.05$  up to 800 mK, for  $B > B^*$  and  $B < B^*$ , while for  $x=0$ , a linearity in  $T^2$  seems to be obeyed only below 500 mK. In these temperature ranges, the magnetization differences can be written as  $\Delta M = \beta(B)T^2$ . Figure 1 and 2 show that  $\beta$  changes from a positive value for  $B < B^*$  to a negative one for  $B > B^*$ , in agreement with the data obtained at higher temperature by an extraction method.<sup>5</sup> It can be noted that the latter data show a small  $T^2$  decrease of  $B^*$  on cooling below 4.2 K, which extrapolates well to the values of  $B^*(T \rightarrow 0)$  of  $\approx 7.7 \text{ T}$  and  $5.2 \text{ T}$ , derived from the present SQUID data for  $x=0$  and  $x=0.05$ , respectively.

The importance of low-temperature measurements has to be stressed, particularly in the case of  $\text{CeRu}_2\text{Si}_2$ . If  $\Delta M$  is forced to obey a  $T^2$  law above 500 mK, the amplitude of  $\beta(B^* \pm \varepsilon)$  drastically decreases, while the width of the anomaly near  $B^*$  increases, as shown by the plots of  $\beta$  vs.  $B$  (Fig. 3). The low-temperature  $T^2$  behavior of  $\Delta M$  follows directly from the thermodynamic Maxwell relation

$$\left. \frac{\partial M}{\partial T} \right|_{P,B} = \left. \frac{\partial S}{\partial B} \right|_P \quad (1)$$

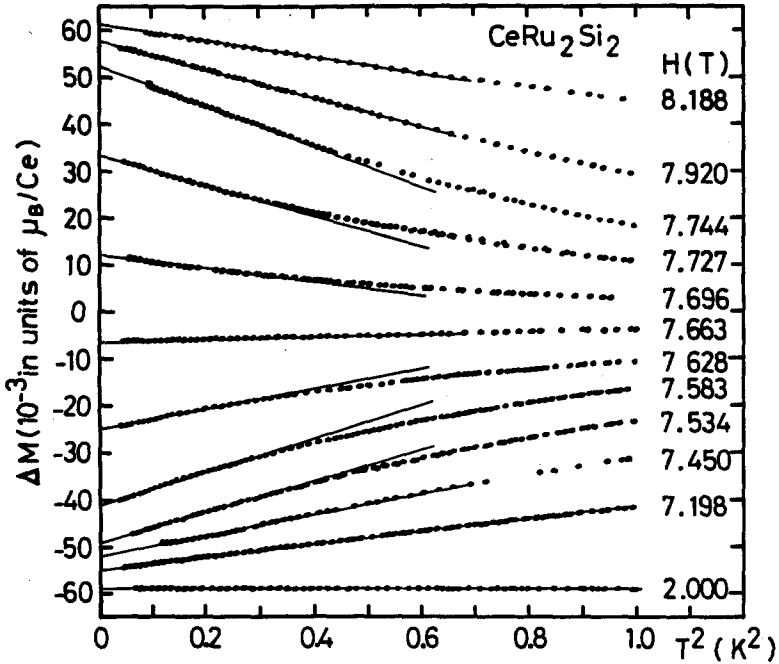


Fig. 1.  $\Delta M = M(B) - M(B^*)$  vs.  $T^2$  for CeRu<sub>2</sub>Si<sub>2</sub> at field as indicated. For sake of clarity the curves have been displaced arbitrary along the vertical axis.

as, in the low-temperature limit, the entropy equals  $\gamma T$ . This allow us to calculate the field dependence of  $\gamma$

$$\frac{\partial \gamma}{\partial B} = 2\beta(B) \quad (2)$$

In the inset of Fig. 3 we show the values for  $\gamma(B^*)$ , calculated from Eq. (2), using different temperature ranges chosen to determine  $\beta(B)$ . The field dependence of  $\gamma$  for  $x = 0$  and  $x = 0.05$  is shown in Fig. 4; for  $x = 0$ ,  $\gamma(B)$  has been calculated from a  $T^2$  fit of  $\Delta M$  for  $T < 500$  mK. We also compare in Fig. 4 the calculated  $\gamma$  values with the limit  $(C/T)_{T \rightarrow 0}$  determined from specific-heat measurements<sup>4</sup> performed down to 350 mK. The metamagnetic transition is much sharper for  $x = 0$  than for  $x = 0.05$ , as shown by the variation of  $\gamma(B)/\gamma(0)$  as a function of the reduced variable  $B/B^*$  (see Fig. 5). The enhancement of  $\gamma$ , that amounts up to 62% at  $B^*$  for CeRu<sub>2</sub>Si<sub>2</sub>, is reduced to 28% for Ce<sub>0.95</sub>La<sub>0.05</sub>Ru<sub>2</sub>Si<sub>2</sub>. Recent specific-heat measurements on our CeRu<sub>2</sub>Si<sub>2</sub> single crystal at high magnetic field in the temperature range  $1.5 \text{ K} \leq T \leq 20 \text{ K}$ , performed by van der Meulen *et al.*,<sup>20</sup> show that the  $\gamma$  term (taken at 1.5 K) drops to  $70 \text{ mJ mol}^{-1} \text{ K}^{-2}$  at 20 T. Magnetization

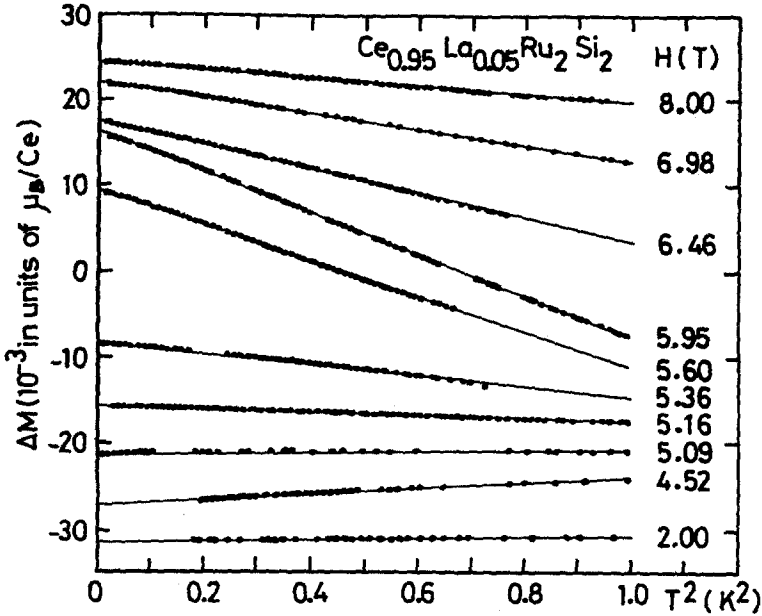


Fig. 2.  $\Delta M = M(B) - M(B^*)$  vs.  $T^2$  for  $\text{Ce}_{0.95}\text{La}_{0.05}\text{Ru}_2\text{Si}_2$  at field as indicated. For sake of clarity the curves have been displaced arbitrary along the vertical axis.

experiments in fields up to 15 T and temperatures down to 1.3 K give a previous estimate of  $\gamma_{1.3\text{K}}$  shown in the insert of Fig. 5, where we fitted the low temperature points to a  $T^2$  law.

For  $x=0$ , the behaviour of  $\gamma$  near the metamagnetic field  $B^*$  seems to mimic a transition through a magnetic instability. In Fig. 6 we present  $\gamma$  (for  $x=0$ ) as a function of the reduced variable  $\delta$ , where  $\delta = (B - B^*)/B$ . Before flattening as  $\delta \rightarrow 0$ ,  $\gamma$  follows a linear  $\sqrt{|\delta|}$  variation with an extrapolation for  $B \rightarrow B^*$  to  $\gamma(B \rightarrow B^*) = 650 \text{ mJ mol}^{-1} \text{ K}^{-2}$  (see inset in Fig. 6). This value is close to the maximum value reached for  $x=0.05$  at  $B^*$  ( $\gamma(B \rightarrow B^*) = 630 \text{ mJ mol}^{-1} \text{ K}^2$ ).  $\gamma(B)$  levels off only for  $(B - B^*)/B^* < 0.01$ , i.e., for  $B = B^* - 800 \text{ Oe}$ .

For the  $\text{CeRu}_2\text{Si}_2$  compound, at low field, a regime change appears in the temperature dependence of the magnetization at constant field (see Fig. 7). This behavior may be characteristic of the presence of impurities (Kondo type) that are weakly coupled to the lattice and easily polarized. This might lead to an initial apparent weak field decrease of  $\gamma(B)$ . In fact, ac susceptibility experiments in zero magnetic field have shown a small peak near 100 mK. When these impurities are fully polarized, the lattice behavior is recovered, i.e., an initial field increase of  $\gamma$ , in accordance with the positive  $T^2$  variation of the initial susceptibility measured between 1.5 K and 4 K.

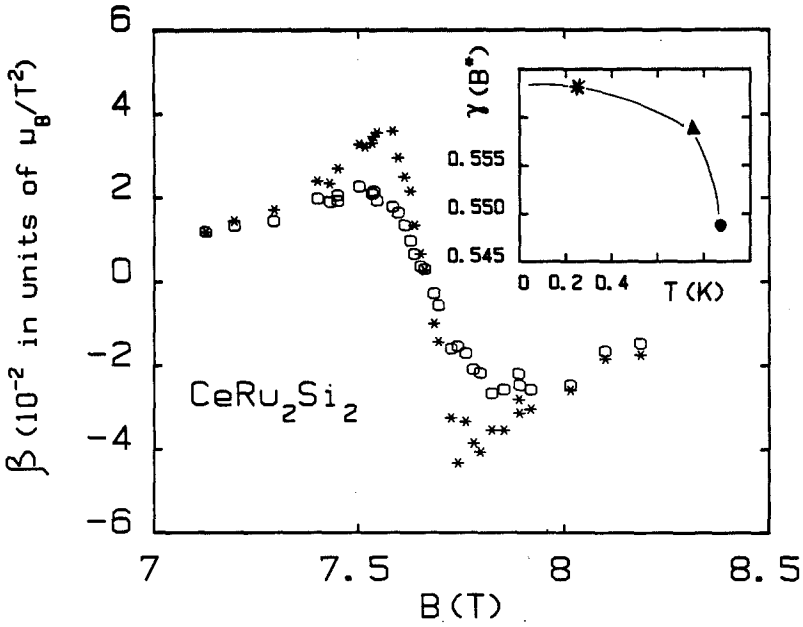


Fig. 3. Field variation of the coefficient  $\beta(B)$  of the  $T^2$  term in the magnetization; (O) and (\*) represent values for  $\beta$  evaluated in the temperature interval 0.5–1.0 K and 0–0.5 K, respectively. The insert shows the corresponding values for  $\gamma(B^*)$  calculated using Eq. (2), where (O) and (\*) are determined in the temperatures ranges as listed above and ( $\blacktriangle$ ) is determined in the interval 0.5–0.75 K.

### 3.2. Thermal Expansion

The coefficient of linear thermal expansion  $\alpha = L^{-1}(dL/dT)$  has been measured along ( $\alpha_{\parallel}$ ) and perpendicular ( $\alpha_{\perp}$ ) to the tetragonal  $c$  axis in both samples in a wide temperature range. The data for  $1.3 \text{ K} < T < 20 \text{ K}$  for different magnetic fields ( $B \parallel c$ ) are plotted in Figs. 8a and 8b for  $x = 0$ , and in Figs. 9a and 9b for  $x = 0.05$ . The corresponding volume expansion is calculated from  $\alpha_v = \alpha_{\parallel} + 2\alpha_{\perp}$ , after smoothing the data for  $\alpha_{\parallel}$  and  $\alpha_{\perp}$  with polynomial fits in selected temperature intervals. Results for  $\alpha_v$  are plotted in Figs. 10a and 10b for  $x = 0$  and  $x = 0.05$ , respectively. As can be observed in Figs. 8 and 9,  $\alpha_{\parallel} \sim 3\alpha_{\perp}$  for  $x = 0$  and  $\alpha_{\parallel} \sim 2.5\alpha_{\perp}$  for  $x = 0.05$ . Assuming an identical proportionality of  $\alpha_{\parallel}$  and  $\alpha_{\perp}$  at lower temperatures, we have measured only  $\alpha_{\parallel}$  below 1 K and calculated the volume expansion by  $\alpha_v = (5/3)\alpha_{\parallel}$  and  $\alpha_v = (9/5)\alpha_{\parallel}$ , for  $x = 0$  and for  $x = 0.05$ , respectively. These low-temperature data are plotted in Fig. 11a and 11b for fields in the vicinity of  $B^*$ .

As follows from Fig. 10,  $\alpha_v$  exhibits a broad maximum in zero magnetic field centered at  $T_m^{\alpha} = 9 \text{ K}$  and  $6 \text{ K}$ , for  $x = 0$  and  $x = 0.05$ , respectively. With

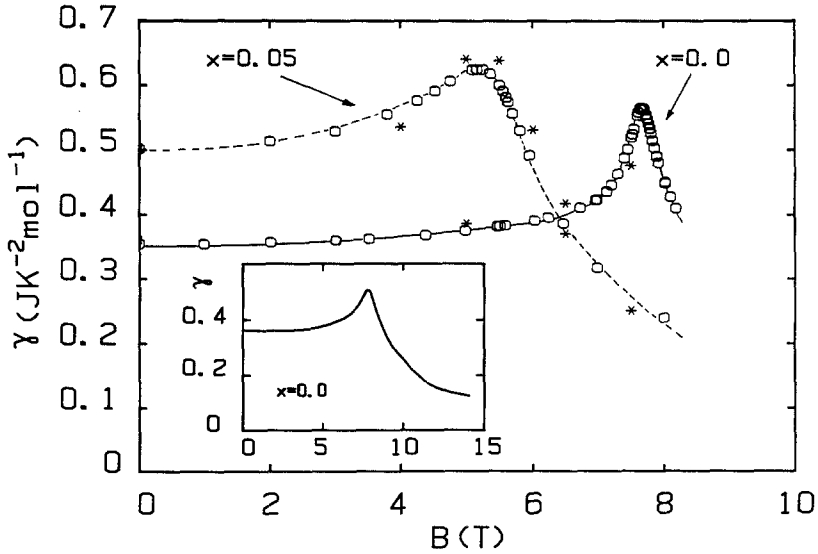


Fig. 4. Field variation of  $\gamma$  calculated from Eq. (2) for  $\text{Ce}_{1-x}\text{La}_x\text{Ru}_2\text{Si}_2$  for  $x=0$  and  $x=0.05$ , as indicated; (\*) are experimental points from Ref. 4. Solid and dashed line are a guide to the eye. The insert shows the field variation of  $\gamma$  calculated from our previous high temperature ( $T < 1.3$  K) susceptibility data (Ref. 15) using Eq. (2).

increasing magnetic field, the anomaly in  $\alpha_v$  shifts towards lower temperatures and becomes negative above  $B^*$ . The change of sign of  $\alpha_v$  at  $B^*$  is directly connected to the occurrence of a maximum in the linear temperature coefficient  $\gamma(B)$  and to the huge pressure variation of  $B^*$ . The low-temperature data (Fig. 11) show that (i) the magnetic field where  $\alpha_v$  changes sign is exactly the same field as that of the maximum of the magnetostriction, and (ii) the temperature  $T_m^\alpha$  has an extremely sharp minimum at  $B \sim B^*$  for the pure system ( $T_m \sim 340$  mK at  $B = 7.685$ ) (see Fig. 12a). The minimum of  $T_m^\alpha$  is less pronounced for the 5% La compound. This effect can be clearly observed in the reduced representation  $T_m(B)/T_m(0)$  as a function of  $B/B^*$  in Fig. 12b.

In Fig. 13 we present the field dependence of the linear coefficient  $a_B (= \alpha_v(B)/T)$  of the volume expansion for the pure and 5% La compound. The maximum enhancement of  $a_B$  just below  $B^*$  for the pure system is more than one order of magnitude larger than for the doped system.

### 3.3. Magnetostriction

In Fig. 14, we present the coefficient of volume magnetostriction  $\lambda'_v = 1/V dV/dB$ , for  $\text{CeRu}_2\text{Si}_2$  at different temperature for  $B \parallel c$ . In previous experiments,<sup>7</sup> we observed that the coefficients  $\lambda'_\parallel$  and  $\lambda'_\perp$  of the linear



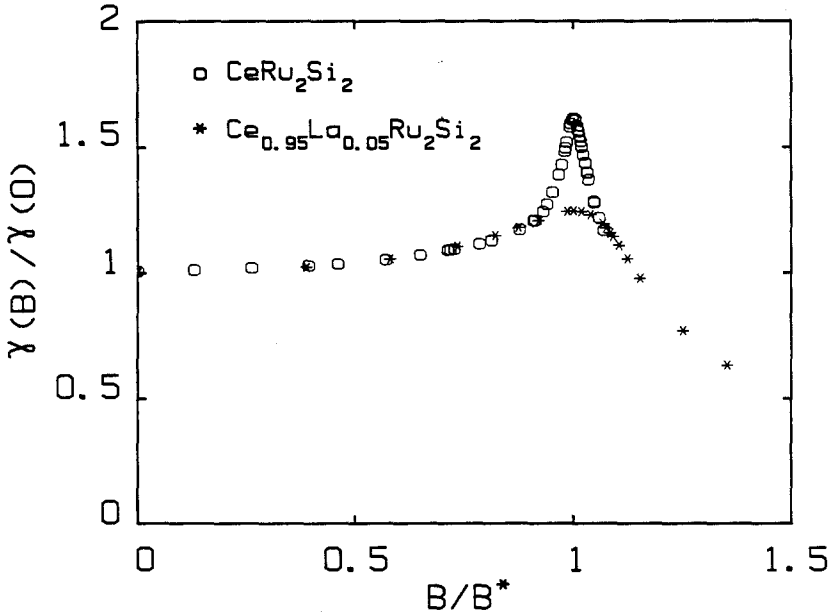


Fig. 5. Relative enhancement  $\gamma(B)/\gamma(0)$  as function of the reduced unit  $B/B^*$  for CeRu<sub>2</sub>Si<sub>2</sub> (○) and for Ce<sub>0.95</sub>La<sub>0.05</sub>Ru<sub>2</sub>Si<sub>2</sub>(\*).

magnetostriction measured parallel and perpendicular to  $B$  follow the relation  $\lambda'_{\parallel} \sim 3\lambda'_{\perp}$ , just as found for the thermal expansion.

Therefore, we have measured in the present experiment only the elongation along the field direction ( $B \parallel c$ ) ( $\lambda'_v = 5/3\lambda'_{\parallel}$ ). The remarkable feature is the large temperature dependence of  $\lambda'_v$  at  $B^*$ . In Fig. 15, we show the field variation of the volume at different temperatures. At  $T \rightarrow 0$ , the volume change occurs in a very narrow field range. The huge volume anomaly at  $B^*$  coincides with the softening of the lattice<sup>17</sup>: 50% for the  $c_{33}$  mode at 60 mK.

For  $x = 0.05$ , the magnetostriction at the metamagnetic transition is smeared out considerably (see inset in Fig. 14). The relative enhancements of  $\lambda'_v$  at  $B^*$  on cooling, for  $x = 0$  and  $x = 0.05$ , are also very different. For CeRu<sub>2</sub>Si<sub>2</sub> $\lambda'_v(340 \text{ mK})/\lambda'_v(1.3 \text{ K}) = 20$ , while for

$$\text{Ce}_{0.95}\text{La}_{0.05}\text{Ru}_2\text{Si}_2\lambda'_v(400 \text{ mK})/\lambda'_v(1.3 \text{ K}) \approx 1.2.$$

#### 4. DISCUSSION

##### 4.1. The Pure Lattice

The main features of our results are (i) the observation of a drastic decrease of the energy scale as  $B \rightarrow B^*$ , thus the necessity to attain very low

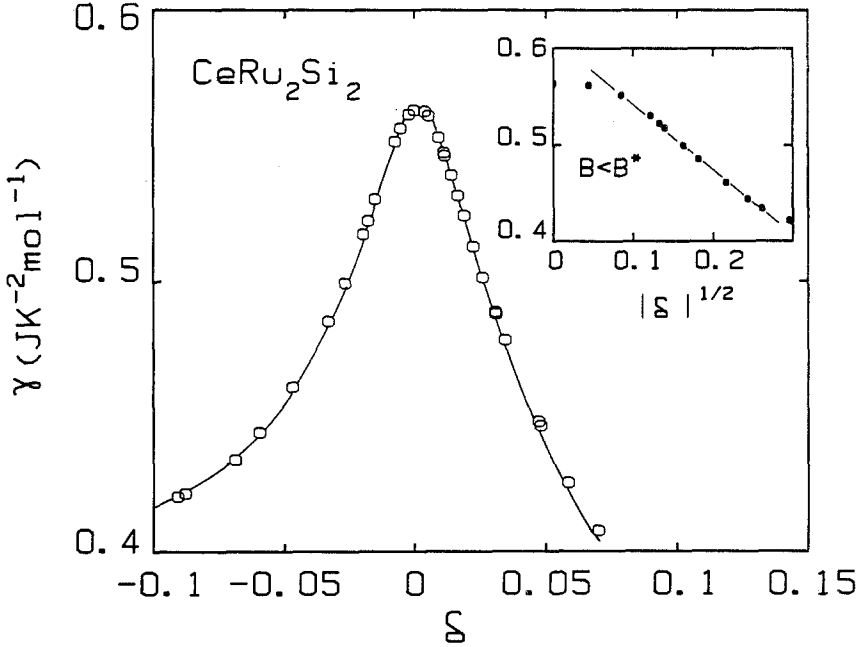


Fig. 6. The  $\gamma$  value calculated from Eq. (2) as a function of  $\delta = (B - B^*)/B^*$  for  $\text{CeRu}_2\text{Si}_2$ . The insert shows the  $\gamma$  value as function of  $|\delta|^{1/2}$  for  $B < B^*$ . The solid lines are a guide to the eye.

temperatures in order to study the transition in the vicinity of the metamagnetic field, (ii) the quasi continuous sweep of the field dependence of  $\gamma$  through  $B^*$ , allowing for a first quantitative measurement of the mass enhancement with field, and (iii) the ability to study the interplay between magnetization, magnetostriction, and electronic low-energy excitations.

Thermal expansion at constant magnetic field is a powerful technique to demonstrate the large field variation of the characteristic temperature, here chosen as  $T_m^\alpha$ . At low temperature  $T < T_m^\alpha$ , a phase diagram ( $B, T_m^\alpha$ ) (Fig. 12a) delimits a low field phase ( $B \leq B^*$ ), where the quasiparticles interact strongly via the intersite magnetic fluctuations of the local  $f$  moment (strongly interacting Fermi liquid), from a high-field phase ( $B > B^*$ ), which corresponds to a polarized localized Fermi liquid. Systematic studies on this polarized phase will give, in the future, unique information on the mass renormalization of heavy-fermion quasiparticles.

In experiments realized above 1 K, the remarkable feature of the metamagnetic transition is its occurrence for a critical value of the magnetization, i.e., the product of the initial susceptibility  $\chi_0$  and the metamagnetic field  $B^*$  is pressure invariant. That leads to develop simple scaling arguments

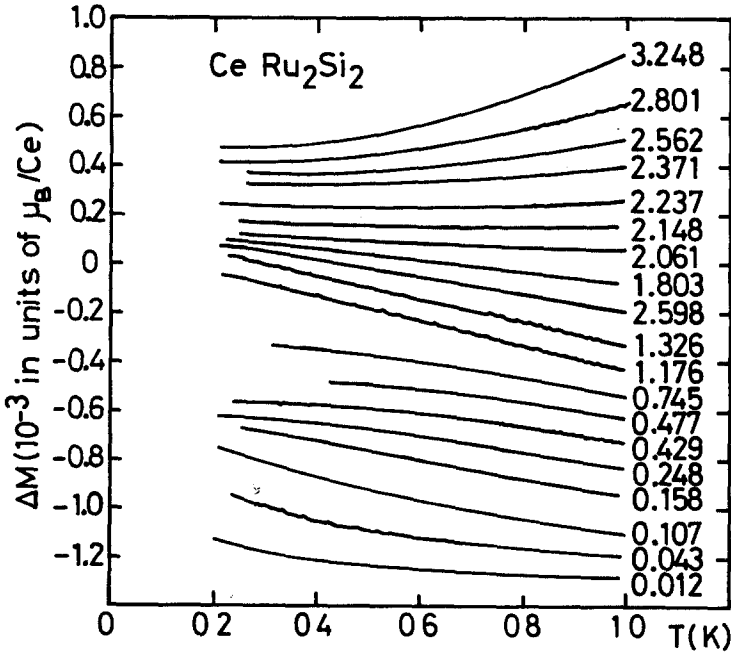


Fig. 7.  $\Delta M = M(B) - M(B^*)$  as a function of  $T$  for CeRu<sub>2</sub>Si<sub>2</sub> for fields  $(B \parallel c) \ll B^*$  as indicated.

to relate variables, as magnetization, compressibility, thermal expansion and magnetostriction. For example, if the entropy can be expressed in the form.

$$S = S\left(\frac{T}{T_S(P)}, \frac{B}{B_S(P)}\right) \tag{3}$$

with only one reduced temperature and field variable, with an identical pressure effective Grüneisen coefficient  $\Omega = \partial \ln T_S / \partial P = \partial \ln B_S / \partial P$ , it can be shown that at low temperature, in an applied field  $B$  where  $\alpha = a_B T$  and  $C = \gamma_B T$ , the linear coefficients are related through the equation

$$a_B = 2 \frac{\Omega}{V_0} \left[ \gamma_B + B \frac{\partial \gamma_B}{\partial B} \right] \tag{4}$$

where  $V_0$  is the molar volume. The slope  $a(B)$  estimated from the linear temperature variation of  $\alpha_v$  and the  $a_{SA}$ , calculated assuming the scaling ansatz of Eq. (3) with the  $\gamma(B)$  term derived from  $\beta(B)$ , are compared in Fig. 16, for  $x=0$  and  $x=0.05$ . The agreement is excellent up to  $B^*$  for  $x=0.05$  and appears less convincing above  $B^*$ . For  $x=0$ , the agreement is good on both side of  $B^*$ , but rather poor in the vicinity of  $B^*$ . This indicates

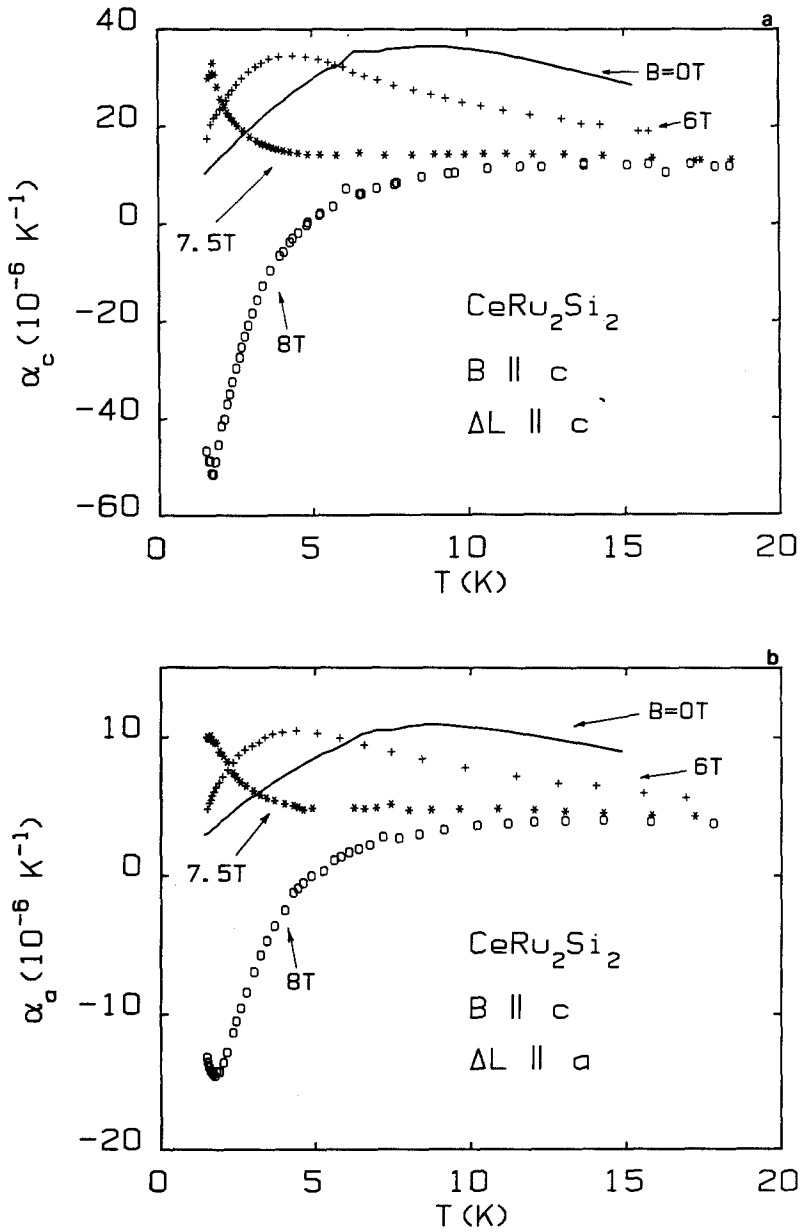


Fig. 8. Coefficient of linear thermal-expansion of  $\text{CeRu}_2\text{Si}_2$  for  $B \parallel c$  in fields of 0, 6, 7.5, and 8 T as indicated: (a)  $\Delta L \parallel c$ , (b)  $\Delta L \parallel a$ .

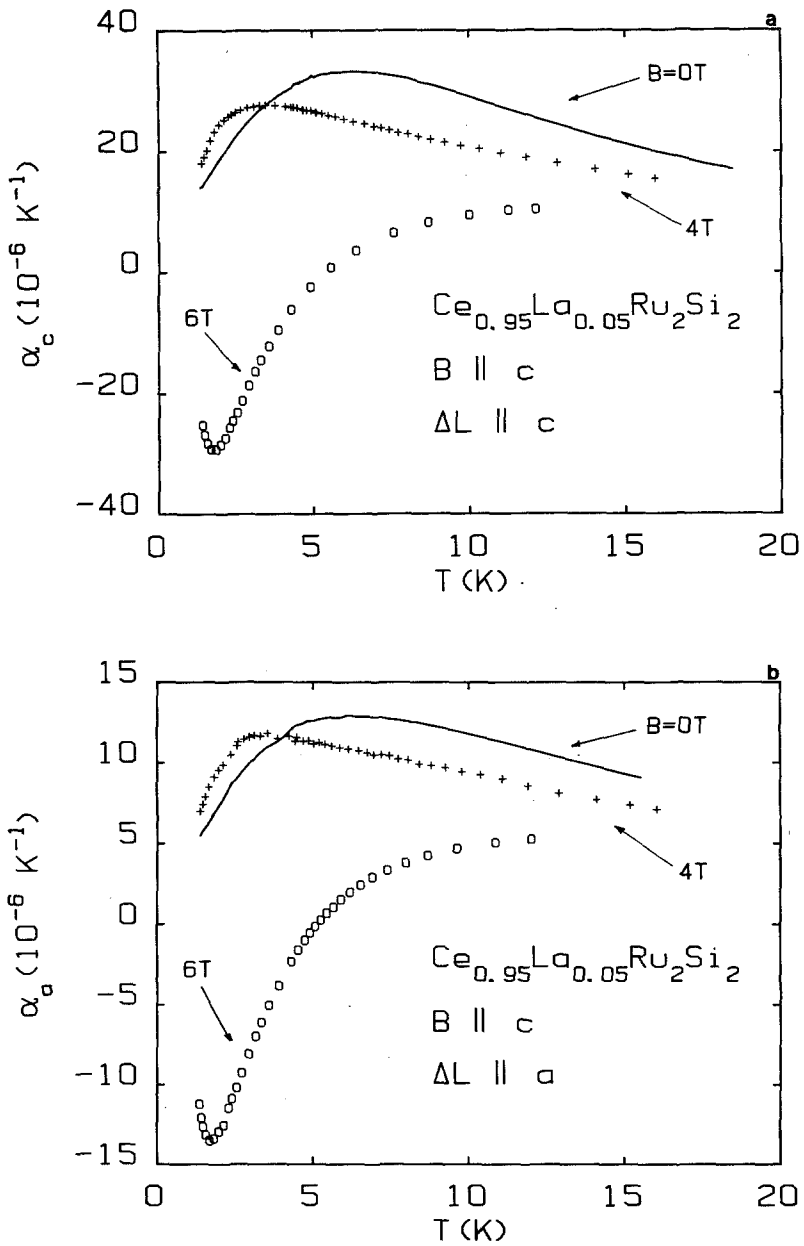


Fig. 9. Coefficient of linear thermal expansion of  $\text{Ce}_{0.95}\text{La}_{0.05}\text{Ru}_2\text{Si}_2$  for  $B \parallel c$  in fields of 0, 4, and 6 T as indicated: (a)  $\Delta L \parallel c$ , (b)  $\Delta L \parallel a$ .

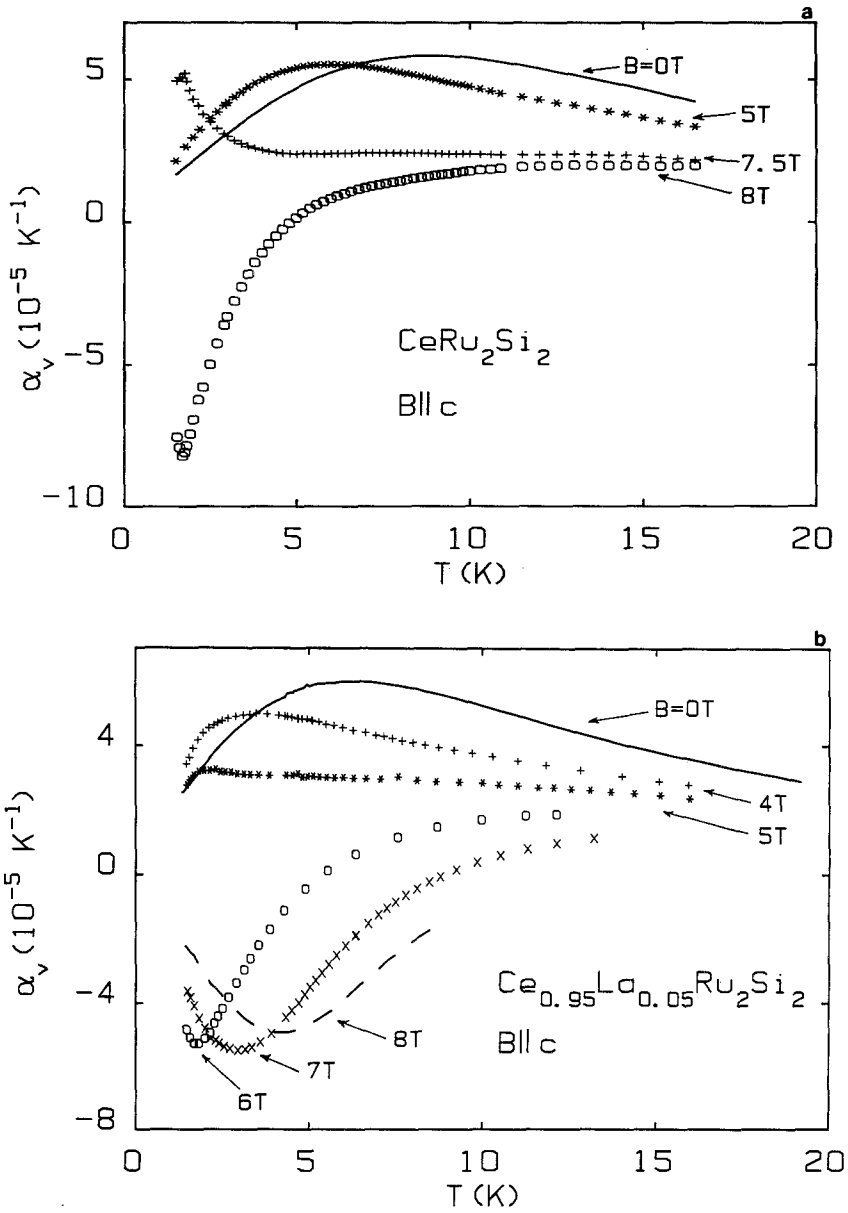


Fig. 10. Coefficient of volume thermal expansion for  $B \parallel c$  in fields as indicated: (a) for  $\text{CeRu}_2\text{Si}_2$ , and (b)  $\text{Ce}_{0.95}\text{La}_{0.05}\text{Ru}_2\text{Si}_2$ .

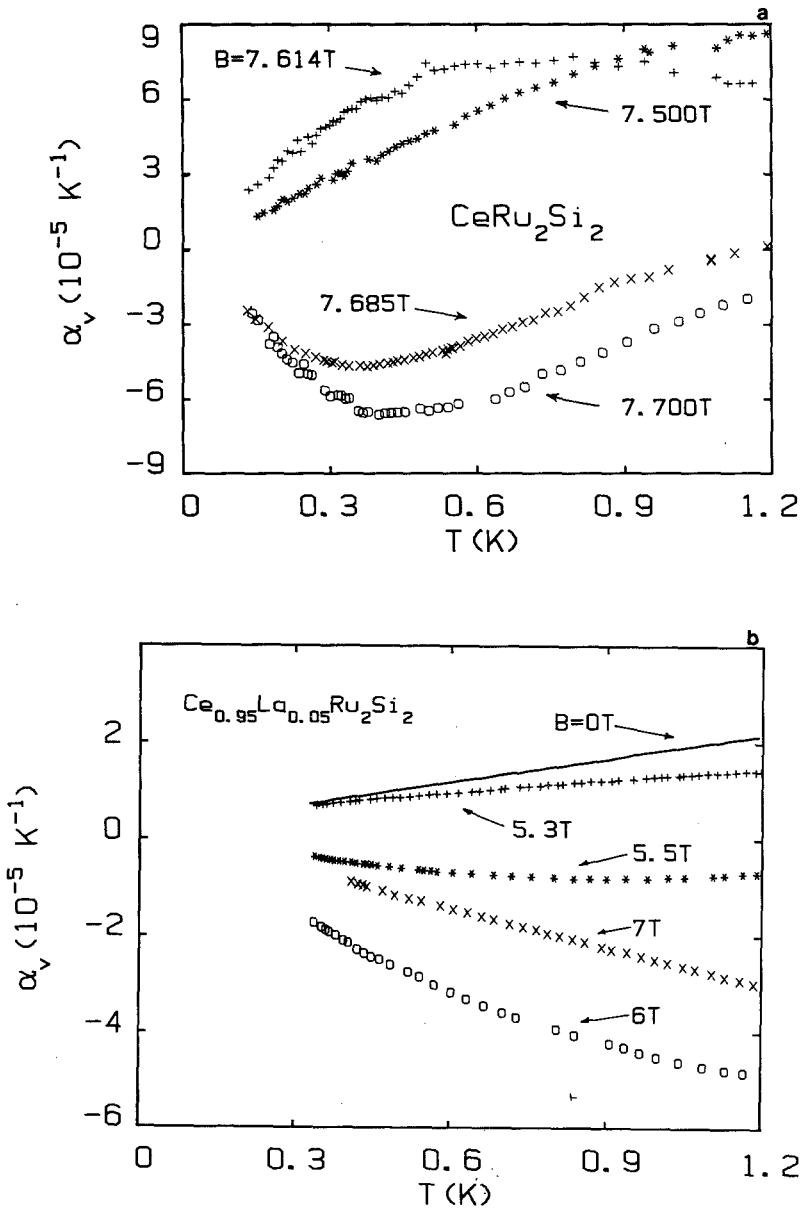


Fig. 11.  $\alpha_v$  for  $B \parallel c$  for fields in the vicinity of  $B^*$  as indicated, (a) for  $\text{CeRu}_2\text{Si}_2$ , and (b)  $\text{Ce}_{0.95}\text{La}_{0.05}\text{Ru}_2\text{Si}_2$ .

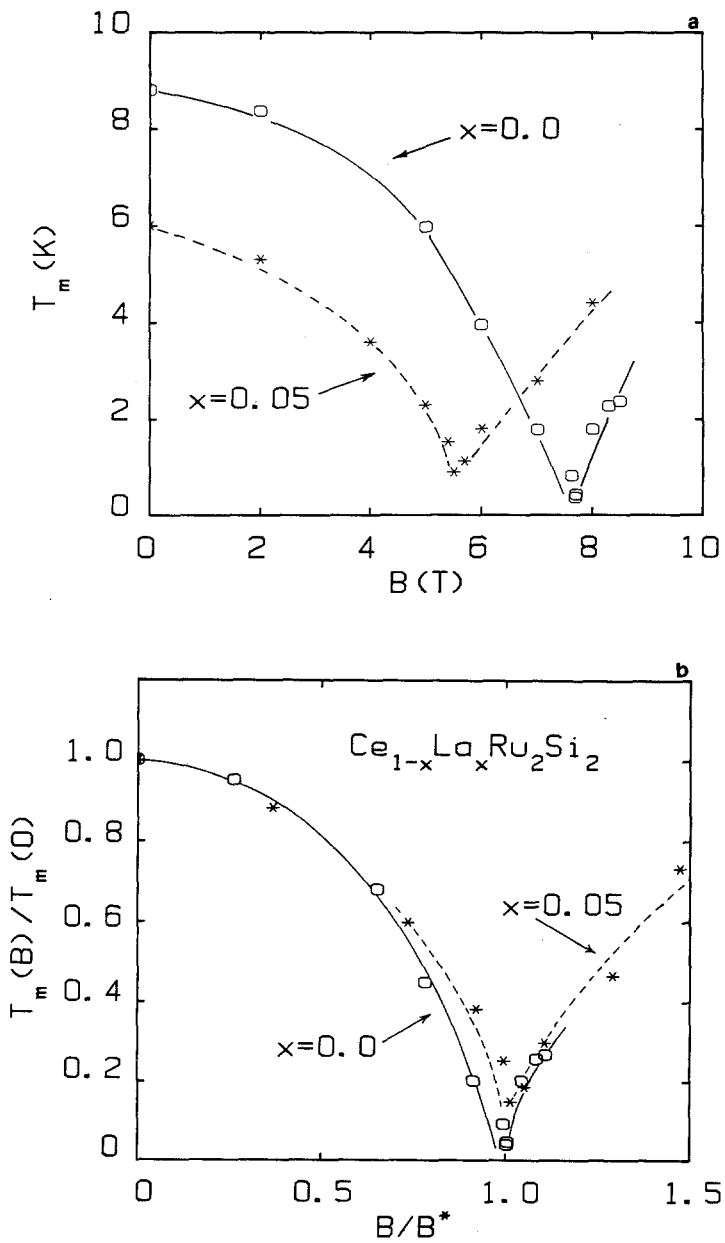


Fig. 12. (a) Field dependence of the temperature  $T_m$  where the extremum in  $\alpha_p$  occurs for  $CeRu_2Si_2$  and  $Ce_{0.95}La_{0.05}Ru_2Si_2$ . (b)  $T_m(B)/T_m(0)$  as function of the reduced unit  $B/B^*$ .



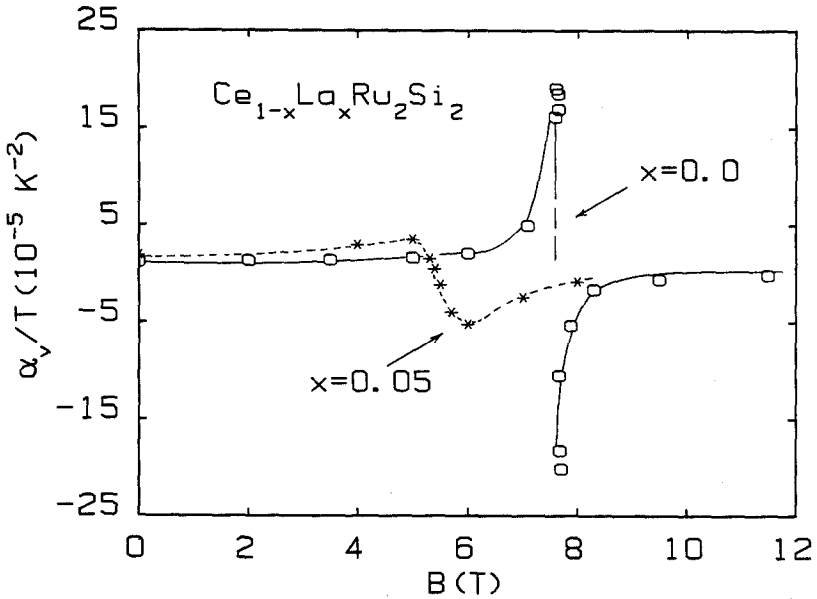


Fig. 13. Field dependence of the linear term  $a(B) = \alpha_v/T$  in the volume expansion for  $B \parallel c$  for  $\text{CeRu}_2\text{Si}_2$  (○) and  $\text{Ce}_{0.95}\text{La}_{0.05}\text{Ru}_2\text{Si}_2$  (\*). Solid lines are guides to the eye.

either the necessity to attain lower temperatures to extract  $\beta(B)$  (i.e.,  $\gamma(B)$  in the vicinity of  $B^*$ ) or a real shortcoming of the scaling ansatz just at  $B^*$ . Above  $B^*$ , for  $x = 0.05$ , the deviation found between  $a(B)$  and  $a_{SA}(B)$  may indicate that when the intersite coupling is destroyed, the inhomogeneity of the alloy (distribution of Kondo temperatures and Grüneisen parameters) appears more clearly in the uncorrelated regime. From our magnetostriction experiments at low temperature, assuming the scaling ansatz, the field dependence of the isothermal compressibility  $\kappa$  and the susceptibility  $\chi_P$ , at constant pressure, can be estimated. Using the thermodynamic relation  $(\chi_P - \chi_v)/\chi_v = (V_0/\kappa)(\lambda_v^2)_{P,T}$ . It is found that the temperature dependence of the susceptibility at constant volume is weak.<sup>16</sup>

The enhancement of  $\gamma$  is well pronounced at  $B^*$ . The occurrence of mass enhancement has first been worked out in resistivity experiments.<sup>5</sup> An enhancement of  $\gamma$  of only 30% could be predicted by comparing at  $B = 0$  and  $B \sim B^*$  the values of the coefficient  $b$  in the linear resistivity between 1.5 and 4.2 K according to a scaling  $b \sim \gamma$ . If a scaling  $A \sim \gamma^2$  is applied to the  $AT^2$  term of the resistivity below 1 K, the correct enhancement of  $\gamma$  is predicted. Thus the apparent mass enhancement decreases on warming. The rapid temperature smearing of the electronic anomaly shows again the necessity to achieve very low temperatures. As mentioned above, before

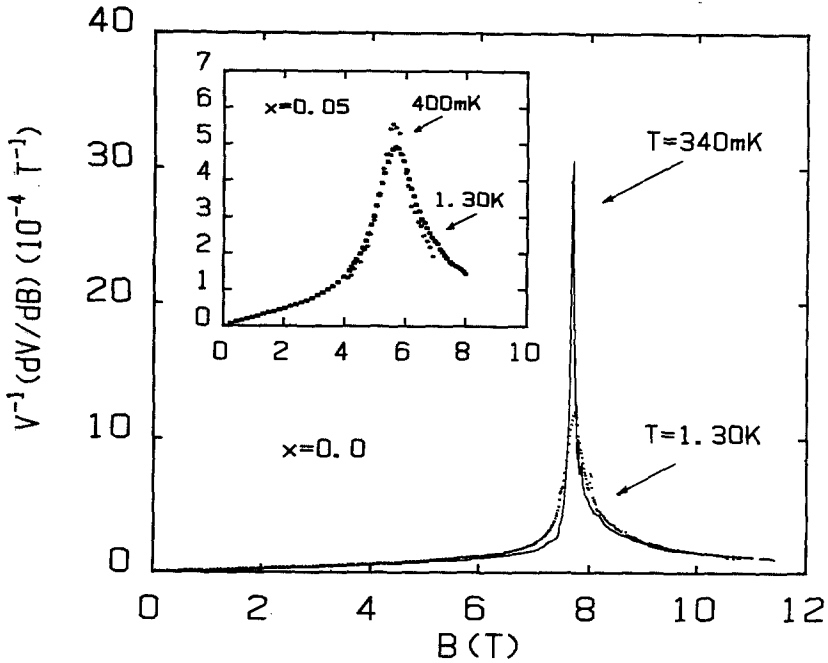


Fig. 14. Coefficient of volume magnetostriction of  $\text{CeRu}_2\text{Si}_2$  for  $B\parallel c$  at temperatures as indicated. The insert shows  $\lambda'_v$  for  $\text{Ce}_{0.95}\text{La}_{0.05}\text{Ru}_2\text{Si}_2$ .

flattening,  $\gamma$  seems to extrapolate to a critical value  $\gamma_c \sim 650 \text{ mJ mol}^{-1} \text{ K}^{-2}$ .  $\gamma_c$  is almost the value reached at  $B^*$  for  $x=0.05$ . Furthermore, in the series of  $\text{Ce}_{1-x}\text{La}_x\text{Ru}_2\text{Si}_2$  (Ref. 4),  $\text{CeRu}_{2-x}\text{Rh}_x\text{Si}_2$  (Ref. 19) or  $\text{CeRu}_2(\text{Si}_{1-x}\text{Ge}_x)_2$  (Ref. 20) the various  $\gamma$  values indicates that  $\gamma_c$  may be a critical value of the appearance of a long-range magnetic order. It is interesting to remark that the self-consistent renormalization theory of weak antiferromagnets<sup>21</sup> predicts a finite maximum of  $\gamma$  as a function of the Stoner factor  $\alpha - 1$  of the staggered susceptibility with a square root dependence in  $\alpha - 1$ .

The magnetic field lowering the Kondo strength leads to the volume expansion and thus to approach the critical volume for the onset of long-range magnetic order. In a simple picture, we expect that local quantum fluctuations prevent the formation of an AF ground state and thus the first-order phase transition characteristic of a usual metamagnetic transition in an antiferromagnet. That corresponds experimentally to the flattening of  $\gamma$  at  $B^*$ .

The role of the disorder is still an open question. For  $x=0$  at  $B=0$  a residual resistivity  $\rho_0 \sim 1.7 \mu\Omega \text{ cm}$  has been measured. It rises up to a maximum value of  $2.8 \mu\Omega \text{ cm}$  at  $B^*$ . The variation of  $\gamma(B^*)$  as a function

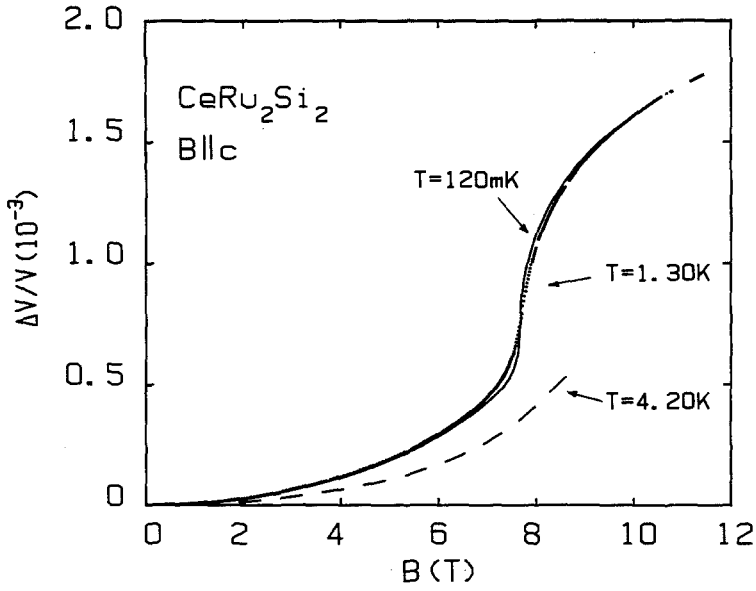


Fig. 15. Volume magnetostriction for  $\text{CeRu}_2\text{Si}_2$  ( $B \parallel c$ ) at the temperatures indicated.

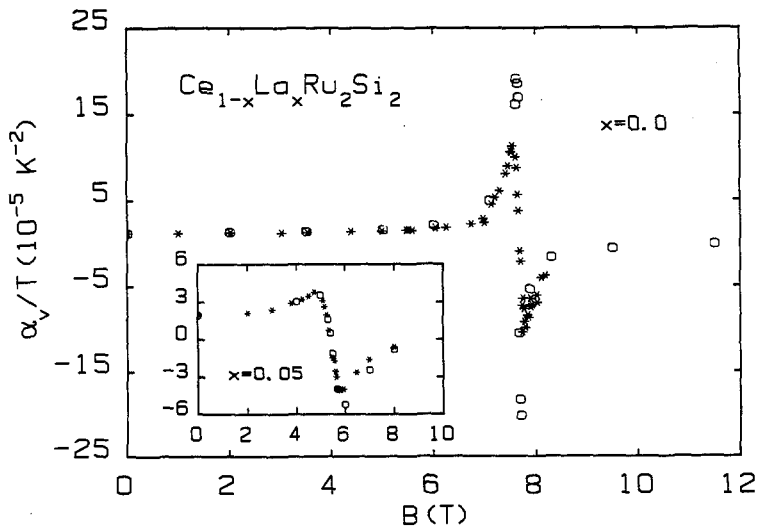


Fig. 16. Field dependence of the linear term  $a(B) = \alpha_v/T$  in the volume expansion for  $B \parallel c$  for  $\text{CeRu}_2\text{Si}_2$ : (O) experimental values (\*), calculated values using Eq. (4). The inset shows the results for  $\text{Ce}_{0.95}\text{La}_{0.05}\text{Ru}_2\text{Si}_2$ .

of  $\rho_0$  must be studied, before taking, into account the claim that the rounding of  $\gamma(B^*)$  is due to quantum fluctuations.

#### 4.2. The Doped Compound ( $x = 0.05$ )

All anomalies measured at  $B^*$  for  $x = 0.05$  appear broadened when compared to the pure lattice case. A classical interpretation of this broadening is to involve the spatial inhomogeneity introduced by substituting Ce atoms by lanthanum atoms. The first effect of doping is to increase the molar volume linearly with  $x$ , inducing a change by a factor  $e^{\Gamma_x x}$  in the characteristic field scale.  $\Gamma_x$  is calculated from  $\Gamma_x = \Gamma(\partial \ln V(x))/\partial x$ . Implicitly this assumes that the local deformation induced by substituting Ce ions by lanthanum ions is transmitted over a large number  $N_c$  of Ce sites. The magnetization  $m_x(B)$  is related to  $m_{x=0}(B)$  through the relation<sup>22</sup>

$$m_x(B) = m_0(Be^{\Gamma_x x}) \quad (5)$$

with  $\Gamma_x \sim 6.7$ . If  $N_c$  is finite, local fluctuations in  $x$  of the order of  $(x(1-x)/N_c)^{1/2}$  must be considered, which will lead to a broadening of all anomalies found for the pure lattice. For example a Dirac peak in  $\chi$  at  $B^*$  for  $x = 0$  will lead to a maximum at  $B_x^*$  with a relative spread  $(\Gamma_x)^2(x)/N_c$ . Figure 17 shows the consequence of finite values of  $N_c$  on the magnetostriction for  $x = 0.05$ , calculated from the data of the pure lattice. At  $T = 0.4$  K the best fit is obtained for  $N_c \sim 400$ . To recover the  $x = 0$  curve, values of  $N_c > 10^5$  are needed, implying a coupling over distances much larger than the antiferromagnetic correlation length, that is limited to the second neighbour distance.<sup>9</sup> Thus the itinerant nature of the quasiparticles must play a leading role in order to realize such a long-range interaction.

#### 4.3. Theoretical Models

In a first approach, lattice and magnetic instabilities should be connected. This idea has recently been put forward in a Kondo collapse model<sup>23</sup> that has been applied to  $\text{CeRu}_2\text{Si}_2$ . The model assumes a ferromagnetic molecular field and a large Grüneisen parameter that enhances the related volume effects. Qualitatively, the enhancement of  $\lambda'_b$  and  $\kappa$  at  $B^*$  can be reproduced. However, the failure of this molecular field approach lies in its unability to reproduce the scaling law  $\chi_0(P)B^*(P) \sim \text{constant}$ . Furthermore, the negligence of intersite spin fluctuations (the mean-field approximation) leads to an enhanced  $\gamma$  value of about 3% above the background value, i.e. more than one order of magnitude smaller than found experimentally.

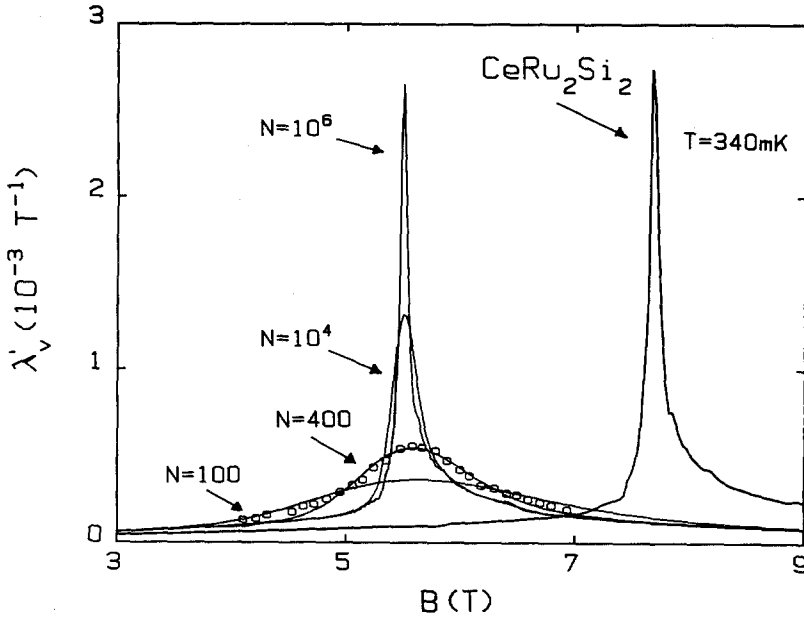


Fig. 17. Comparison of the coefficient of volume magnetostriction ( $B\parallel c$ ) for  $\text{Ce}_{0.95}\text{La}_{0.05}\text{Ru}_2\text{Si}_2$  as measured at 400 mK ( $\circ$ ) and as calculated for different values of  $N$  using the data for pure  $\text{CeRu}_2\text{Si}_2$  at 340 mK (the small temperature difference is neglected).

Recently, a new quantum phenomenological model<sup>24</sup> has been formulated for heavy-fermion systems. This model takes into account simultaneously the localized spin fluctuations (as observed in neutron scattering experiments) and the itinerant fermion quasiparticles. It incorporates the usual RKKY interaction between the localized moments and takes into account the nonlinear effects of the spin polarization. This elaborate model seems powerful to understand metamagnetism and weak antiferromagnetism with tiny ordered moment. Both phenomena are clearly highly sensitive to doping. The experimental scaling law  $\chi_0(P)B^*(P) = \text{constant}$  is recovered in the case of metamagnetism. The magnetization process in heavy-fermion systems<sup>25</sup> has also been studied in a model of weakly interacting Kondo centers. Rather large values of the effective Kondo temperature and of the intersite ferromagnetic coupling constant are needed. Using a one-dimensional Kondo lattice without orbital degeneracy (with a treatment beyond the mean-field level), it can be shown that the intersite correlations are not rigid but change rapidly as the system is magnetized. None of these models consider the feedback with the volume instability yet.

Experimentally, there is now the need to perform new inelastic neutron-scattering measurements. The collapse of AF correlations at  $B^*$  has only been studied above 1.5 K, i.e., far above  $T_m^\alpha(B^*) \sim 340$  mK for  $x=0$ . Ferromagnetic correlations seem to exist, comparing bulk magnetization experiments and time of flight inelastic neutron scattering data.<sup>26</sup> In a next experimental study, the field variation of the ferromagnetic and anti-ferromagnetic fluctuations below  $T_m^\alpha(B^*)$  should be investigated.

## 5. CONCLUSIONS

Quantitative measurements have been realized on the mass enhancement in  $Ce_{1-x}La_xRu_2Si_2$  via magnetization measurements. The results strongly suggest that pure  $CeRu_2Si_2$  approaches a magnetic instability at  $B^*$  for  $T \rightarrow 0$ . We underline the interplay between the magnetization, the volume variation and the electronic properties and the necessity to take into account intersite magnetic fluctuations. The rapid smearing out of all properties ( $\gamma, \lambda'_v, \chi_B$  at  $B^*$ ) on doping shows the importance of the homogeneity of the sample connected with the itinerant nature of the heavy quasiparticles. This strongly suggests that metamagnetism and small ordered moment in heavy fermion compounds must be considered within the same approach.

## Acknowledgments

A.L. is supported by Concelho Nacional de Desenvolvimento Científico e Tecnológico, Brazil. The work of A.d.V. has been made possible by a fellowship of the Royal Netherlands Academy of Arts and Sciences.

## REFERENCES

1. J. Flouquet, J. C. Lasjaunias, J. Peyrard, and M. Ribault, *J. Appl. Phys.* **53**, 2127 (1983).
2. D. Jaccard and J. Flouquet, *J. Magn. Magn. Mater.* **47&48**, 45 (1985).
3. M. J. Besnus, P. Lehmann, J. P. Kappler, and A. Meyer, *Solid State Commun.* **55**, 779 (1985).
4. R. A. Fisher, N. E. Phillips, C. Marcenat, J. Flouquet, P. Haen, P. Lejay, and J. M. Mignot, *J. Phys. (Paris)* **49**, C8-759 (1988). R. A. Fisher, C. Marcenat, N. E. Phillips, J. Voiron, P. Haen, F. Lapierre, P. Lejay, and J. Flouquet (to be published), and references therein.
5. P. Haen, J. Flouquet, F. Lapierre, P. Lejay, and G. Remenyi, *J. Low Temp. Phys.* **67**, 391 (1987).
6. J. M. Mignot, J. Flouquet, P. Haen, F. Lapierre, L. Puech, and J. Voiron, *J. Magn. Magn. Mater.* **76&77**, 97 (1988).
7. A. Lacerda, A. de Visser, P. Haen, P. Lejay, and J. Flouquet, *Phys. Rev. B* **40**, 8759 (1989).
8. S. Quezel, P. Burlet, J. L. Jaccard, L. P. Regnault, J. Rossat-Mignod, C. Vettier, P. Lejay, and J. Flouquet, *J. Magn. Magn. Mater.* **76&77**, 403 (1988).
9. J. Rossat-Mignod, L. P. Regnault, J. L. Jaccoud, C. Vettier, P. Lejay, J. Flouquet, E. Walker, D. Jaccard, and A. Amato, *J. Magn. Magn. Mater.* **76&77**, 376 (1988).

10. J. J. M. Franse, A. de Visser, A. Menovsky, and P. H. Frings, *J. Magn. Magn. Mater.* **52**, 61 (1985).
11. A. de Visser, F. R. de Boer, A. A. Menovsky, and J. J. M. Franse, *Solid State Commun.* **64**, 527 (1987).
12. C. Paulsen, A. Lacerda, A. de Visser, K. Bakker, L. Puech, and J. L. Tholence, in *The Proceedings of the Yamada Conference XXV on Magnetic Phase Transition, Osaka, April 13-16, 1990*. (to be published).
13. C. Paulsen, A. Lacerda, J. L. Tholence and J. Flouquet, in *The Proceedings of the XIX Conference on Low Temperatures Physics, Brighton, August 16-22, 1990*. (to be published).
14. A. de Visser, Ph.D. Thesis, University of Amsterdam, 1986.
15. A. Lacerda, A. de Visser, L. Puech, P. Lejay, P. Haen, J. Flouquet, J. Voiron, and F. J. Ohkawa, *Phys. Rev. B* **40**, 11429 (1989).
16. A. Lacerda, A. de Visser, L. Puech, P. Lejay, P. Haen, and J. Flouquet, *J. Appl. Phys.* **67**, 5212 (1990).
17. G. Bruls *et al.*, to be published.
18. L. Puech, J. M. Mignot, P. Lejay, P. Haen, J. Flouquet, and J. Voiron, *J. Low Temp. Phys.* **70**, 237 (1988).
19. B. Lloret, B. Chevallier, B. Buffat, J. Etourneau, S. Quezel, A. Lamharrar, J. Rossat-Mignod, R. Calemczuk, and E. Bonjour, *J. Magn. Magn. Mater.* **63&64**, 85 (1987); R. Calemczuk, E. Bonjour, J. Rossat-Mignod, and B. Chevallier, in *The Proceedings of the Yamada Conference XXV on Magnetic Phase Transition, Osaka, April 13-16, 1990*. (to be published).
20. J. S. Kim, B. Andraka, G. Fraunberger, and G. R. Stewart, *Phys. Rev. B* **41**, 541 (1990).
21. T. Moriya, in *Spin Fluctuation in Itinerant Electron Magnetism* (Springer-Verlag, Berlin, 1985).
22. L. Puech *et al.*, to be published.
23. F. J. Ohkawa, *Solid State Commun.* **71**, 907 (1989).
24. K. Miyake and Y. Kuramoto, in *The Proceedings of the Yamada Conference XXV on Magnetic Phase Transition, Osaka, April 13-16, 1990* (to be published).
25. K. Ueda, K. Yamamoto, and R. Konno, in *The Proceedings of the Yamada Conference XXV on Magnetic Phase Transition, Osaka, April 13-16, 1990*. (to be published).
26. A. Severing, E. Holland-Moritz, and B. Frick, *Phys. Rev. B* **39**, 4164 (1989).